# DEVELOPMENT OF COMPACT GAS-LIQUID SEPARATOR USING SURFACE TENSION

*Naoki Shikazono, Department of Mechanical Engineering, The University of Tokyo, Hongo 7-3-1, Bunkyo-ku, Tokyo 113-8656, Japan*
*Ryuhei Azuma, Department of Mechanical Engineering, The University of Tokyo, Hongo 7-3-1, Bunkyo-ku, Tokyo 113-8656, Japan*
*Tomoaki Sameshima, Department of Mechanical Engineering, The University of Tokyo, Hongo 7-3-1, Bunkyo-ku, Tokyo 113-8656, Japan*
*Hiroshi Iwata, Nichirei Industries Co. Ltd., Mayumi 1570, Ohhira-machi, Tochigi-ken 329-4415, Japan*

**Abstract:** In the present study, a compact gas-liquid separator using surface tension is proposed and its performance is evaluated. The gas bubbles are forced out from the micro grooves at the expanding section by the minimization effect of excess gas-liquid interface free energy, while the liquid phase remains confined inside the micro grooves. Two major limits of gas-liquid separation, i.e., (1) flooding limit at high liquid flow rate, and (2) entrainment limit at high gas flow rate are found and investigated. Dimensionless correlations for predicting gas-liquid separation limits are proposed. Then, a series of 4-16kW capacity gas-liquid separators for practical R410A air conditioning system are developed. The volume of the separator is about 1/7 compared to the conventional separators. Pressure drop reduction by by-passing the gas from the evaporator is demonstrated in the real R410A cycle.

*Key Words: Two-phase Flow, Heat Pump, Surface Tension, Gas-liquid Separator, Micro Grooves*

## 1 INTRODUCTION

It is widely accepted that heat pump technology is one of the most promising technologies for reducing energy consumption and $CO_2$ emission of civilian and industrial sectors. However, efficiencies of component technologies, e.g., compressor, motor, heat exchanger, fan, etc., are already considerably high, and further improvement is considered to be extremely difficult. Efficient cycles such as dual compression cycle, ejector cycle and gas-bypass cycle are expected, but their cost must be further reduced before widely introduced into the market.

Gas-liquid separator is one of the basic components used in such efficient cycles. Conventional gas-liquid separators are based on volume forces such as gravitational or centrifugal forces. Although structure of those separators based on volume forces are simple, it is difficult to reduce the total volume. In addition, postural limitations sometimes exist for the installation. Instead of using body forces, separator using surface force is expected to possess a possibility of reducing the size. Asano et al. [1, 2] investigated Y shaped junction as a gas-liquid separator. It is reported that perfect separation was achieved at intermittent flows, but its performance was very sensitive to the inlet flow patterns. In the present study, a compact gas-liquid separator using surface tension is proposed and its performance is evaluated. The gas bubbles are forced out from the micro grooves at the expanding section by the minimization effect of the excess gas-liquid interface free energy, while the liquid phase remains confined inside the micro grooves. The limits of gas-liquid separation are investigated by air-water experiment and dimensionless correlations for predicting gas-liquid separation limits are proposed. Finally, a series of 4-16kW capacity gas-liquid separators for R410A system are developed. The basic characteristics of these separators when used in refrigerant cycle are investigated.

## 2 AIR-WATER EXPERIMENT

### 2.1 Experimental procedure

Figure 1 shows the gas-liquid separator used in the air-water experiment. The test section is basically axisymmetric. Air and water flow in from the inlet 1 and introduced through the porous

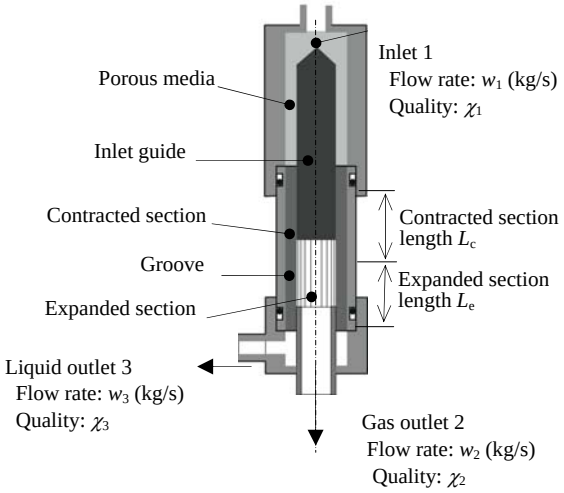


Fig.1 Schematic of the Gas-Liquid Separator

Table 1 Specification of the test section

| Cross section shape | | Triangle | Triangle | Trapezoid |
|---|---|---|---|---|
| Groove pitch $b$ | (mm) | 1.3 | 2.0 | 1.3 |
| Groove hydraulic diameter $D_h$ | (mm) | 0.83 | 1.24 | 1.28 |
| Groove cross section area $A_c$ | ($mm^2$) | 0.99 | 2.24 | 1.74 |
| Crest diameter $D_i$ | (mm) | 6.4 | 9.5 | 6.4 |
| Base diameter $D_o$ | (mm) | 9.4 | 14.1 | 9.4 |
| Contracted section length $L_c$ | (mm) | 42 | 62 | 63 |
| Expanded section length $L_e$ | (mm) | 15, 29 | 44 | 29 |
| Gas outlet pipe thickness $t$ | (mm) | 0.9 | 1.3 | 0.9 |

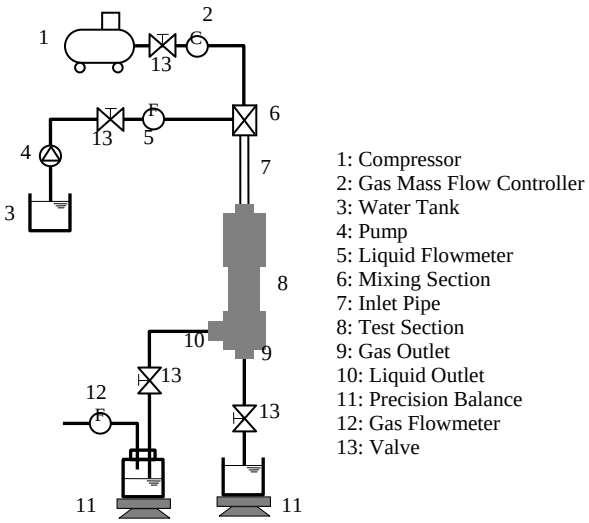


Fig. 2 Experimental setup

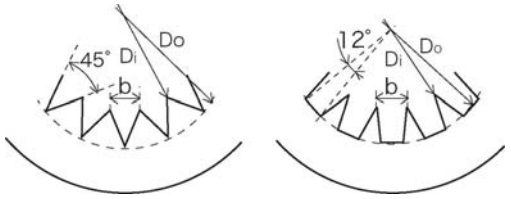


(a) Triangular groove (b) Trapezoidal groove

Fig. 3 Groove cross section

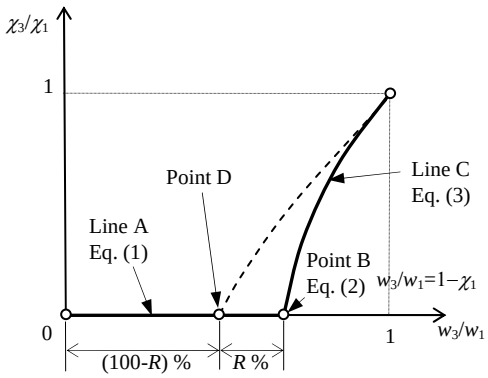


Fig. 4 Gas-liquid separation line

distributor to the contracted region. Then, the flow is introduced to the expansion region where the gas bubbles are forced out from the micro grooves while the liquid phase remains confined inside the micro grooves. Air and liquid phases flow out from exits 2 and 3, respectively. In the present study, the diameters of inlet guide and gas outlet tube are kept same as the groove inner diameter $D_i$, and the length of the contracted region is set equal to 50 times of the hydraulic diameter of each groove.

Figure 2 shows the experimental setup. Air and water are mixed and introduced from the test section. Flow rates at the two exits are controlled by the two valves. Water flow rates were measured by precision balances, and air flow rate was measured by the mass flow meter. Three different grooves are tested as shown in Table 1 and Fig. 3. Triangular grooves with groove width $b$ = 1.3 mm and 2 mm, trapezoidal groove with width $b$ = 1.3 mm are tested. Expansion region lengths were set either as $L_e$ = 2.3 $D_i$ or 4.6 $D_i$ for $b$ = 1.3 mm triangular groove. For other grooves, $L_e$ was set as 4.6 $D_i$. The inner surface of the test section was painted by a hydrophilic paint, and the measured contact angle was 15～20° .

As shown in Fig. 1, two phase flow of mass flow rate $w_1$ and quality $\chi_1$ flows inside inlet 1. And the mass flow rates and qualities of exits 2 and 3 are $w_2$, $w_3$ and $\chi_2$, $\chi_3$, respectively. Figure 4 shows the

gas liquid separation line. Horizontal axis is the flow rate ratio $w_3/w_1$ and the vertical axis is the quality ratio $\chi_3/\chi_1$. Equation (1) represents the case at which only liquid phase flows out from the exit 3 (line A). Equation (2), which corresponds to point B in Fig. 4, represents the perfect separation point where all liquid flows out from exit 3 and all gas flows out from exit 2. Equation (3) represents line C where no liquid flows out from exit 2. The line A → point B → line C is defined as perfect separation line. When $w_3/w_1$ is varied from 0 to 1, exit quality $\chi_3/\chi_1$ must trace this perfect separation line. As is apparent from its definition, the perfect separation line is a function of inlet quality $\chi_1$.

$$\chi_3/\chi_1 = 0 \qquad (0 < w_3/w_1 < 1-\chi_1) \tag{1}$$

$$\chi_3/\chi_1 = 0 \qquad (w_3/w_1 = 1-\chi_1) \tag{2}$$

$$\frac{\chi_3}{\chi_1} = \frac{1}{\chi_1} + \frac{w_1}{w_3}\left(1-\frac{1}{\chi_1}\right) \quad \left(1-\chi_1 < \frac{w_3}{w_1} < 1\right) \tag{3}$$

In order to evaluate the gas-liquid separation characteristics, it is necessary to quantify the deviation from this perfect separation line. When separation is imperfect, separation line becomes like the dashed line shown in Fig. 4. The flow rate $(w_3/w_1)_D$ at point D is the maximum flow rate at which gas starts to flow out from exit 3. The flow rate $(w_3/w_1)_D$ at point D is smaller than the flow rate at point B ($w_3/w_1$=1-$\chi_1$). At point D, the ratio of liquid phase which flowed out from exit 2 is expressed as;

$$R = \left(1-\frac{(w_3/w_1)_D}{1-\chi_1}\right)\times 100 \quad (\%) \tag{4}$$

We define $R$ (%) as the liquid non-recovery rate. As shown in Fig. 4, $R$ is equal to the ratio of the distances B-D and B-O. During the experiment, maximum flow rate $w_3/w_1$ at which 1% of the gas flows out from exit 3 is measured, and the liquid non-recovery rate $R$ is calculated using Eq. (4). In the present study, perfect gas liquid separation is defined as the case when $R \leqq 1$ (%) is achieved.

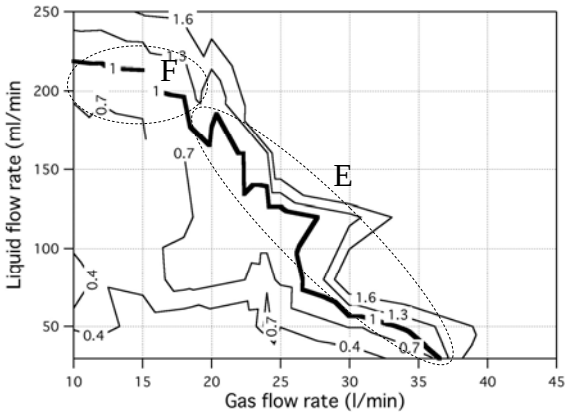


(a) Triangular groove $b$ = 1.3 mm

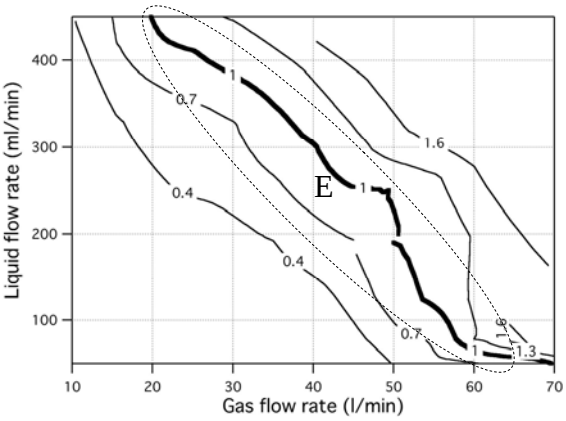


(b) Triangular groove $b$ = 2.0 mm

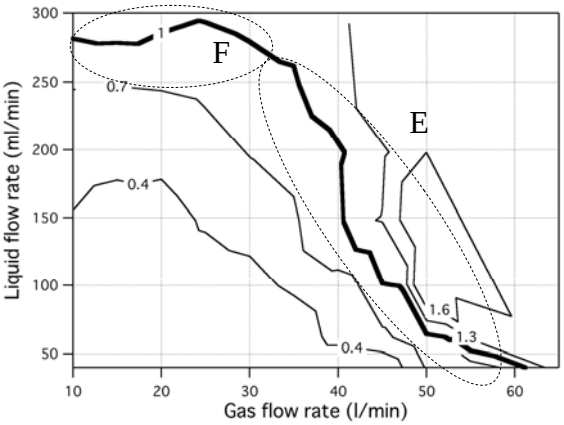


(c) Trapezoidal groove $b$ = 1.3 mm

Fig. 5 Liquid non-recovery rate for $L_e = 4.6D_i$

## 2.2 Experimental results

Figure 5 shows the contour map of the measured liquid non-recovery rate $R$ for $L_e$=4.6$D_i$ case. Horizontal axis is the air flow rate, and the vertical axis is the liquid flow rate. The thick line in Fig. 5

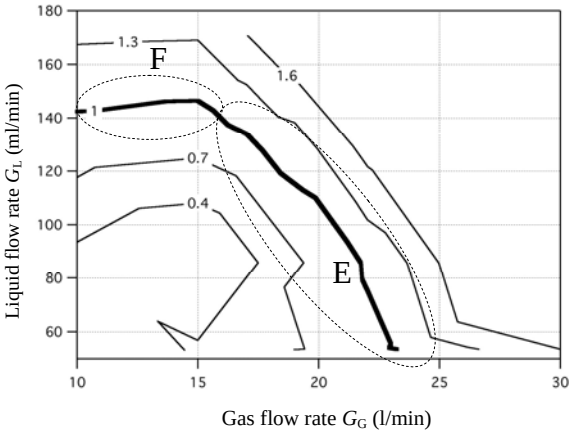


Fig. 6 Liquid non-recovery rate for $b$ = 1.3 mm, $L_e = 2.3D_i$

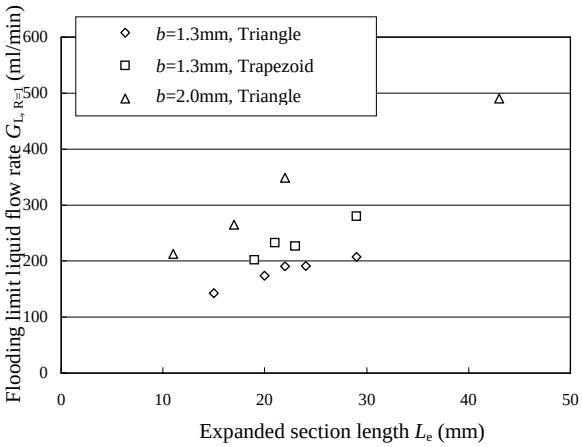


Fig. 7 Flooding limit liquid flow rate

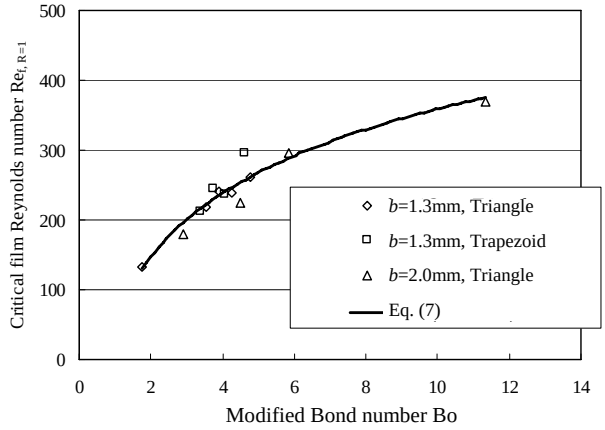


Fig.8 Correlation for the flooding limit

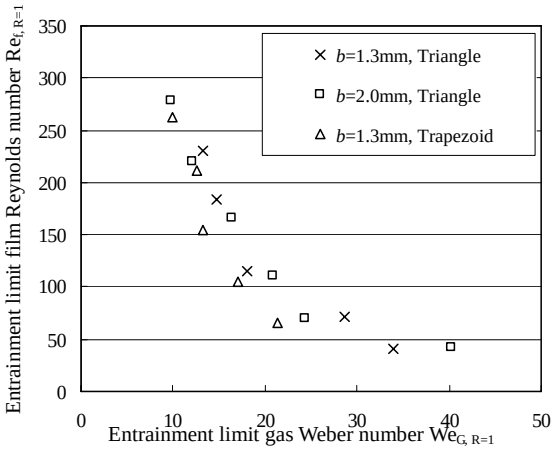


Fig. 9 Correlation for the entrainment limit

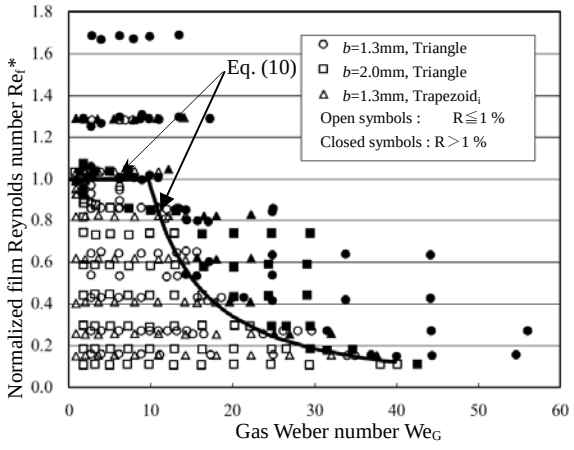


Fig. 10 Correlation for gas-liquid separation limit

represents the $R$ = 1 (%) border. Two major limits of gas-liquid separation, i.e., flooding limit at high liquid flow rate (region F in Fig. 5), and entrainment limit at high gas flow rate (region E in Fig. 5) are observed. It is apparent from Fig. 5 that gas liquid separation depends strongly on groove dimension.

Figure 6 shows the triangular groove with $b$ = 1.3 mm and $L_e$=3.2$D_i$ case. Compared with Fig. 5(a), it is interesting to note that the length of the expansion region has a strong effect especially on the separation limit. Gas-liquid separation is degraded for shorter $L_e$. Thus, $L_e$ was varied in order to investigate the effect of expansion region length on the flooding limit. Liquid flow rates at the flooding limit are plotted against expansion length in Fig. 7. Flooding limit increases with expansion length. From flow visualization, it is observed that flow fluctuation makes the groove flooded and the waves of the liquid flow is the cause of the flooding limit. It is considered that the potential of accumulating this fluctuation depends on the open volume of the groove which is negatively correlated to the capillary pumping ability of the grooves. Thus, modified Bond number

$$\mathrm{Bo} = \frac{\rho_L g L_e}{\sigma / b} \tag{5}$$

is introduced. Film Reynolds number is known to be the important parameter for scaling falling film thickness:

$$\mathrm{Re}_f = \frac{4\rho_L G_L}{\mu_L L_{groove}} \tag{6}$$

where $L_{groove}$ is the perimeter length of the grooves. The critical film Reynolds number at which flooding takes place is plotted against modified Bond number in Fig. 10. It can be seen from the figure that flooding limit is well correlated by the modified Bond number. From the present results, following dimensionless correlation for the flooding limit is obtained.

$$\mathrm{Re}_{f,R=1} = 130.0 \ln(\mathrm{Bo}) + 56.3 \tag{7}$$

For the entrainment limit, gas Weber number is introduced to express the inertial and surface tension effects.

$$\mathrm{We}_G = \frac{\rho_G j_{G,c}{}^2 b}{\sigma} \tag{8}$$

where $j_{G,c}$ is the gas superficial velocity inside the groove. Figure 9 shows the entrainment limit as a function of film Reynolds number and gas Weber number. As shown in the figure, entrainment limit can be well correlated by these two dimensionless numbers.

In order to express both flooding and entrainment limits, film Reynolds number, Eq. (6), is normalized by Eq. (7) as:

$$\mathrm{Re}_f^* = \frac{\mathrm{Re}_f}{130.0\ln(\mathrm{Bo}) + 56.3} \tag{9}$$

Figure 10 shows whole experimental data plotted against gas Weber number and normalized film Reynolds number, Eq. (9). All the data can be scaled very well by these parameters regardless of groove dimension and expansion length. Finally,

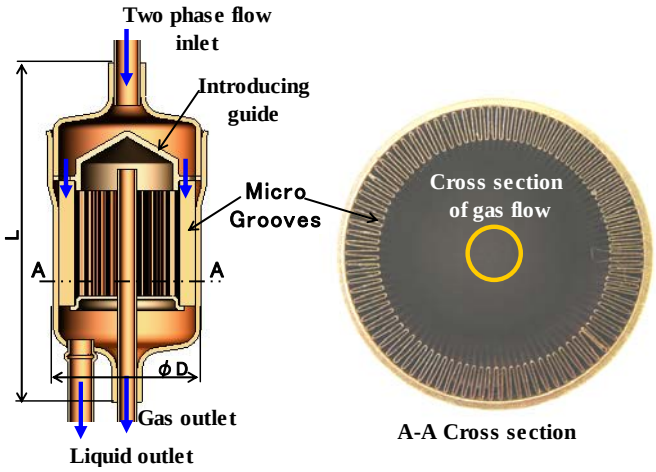


Fig. 11 Developed gas-liquid separator fro R410A

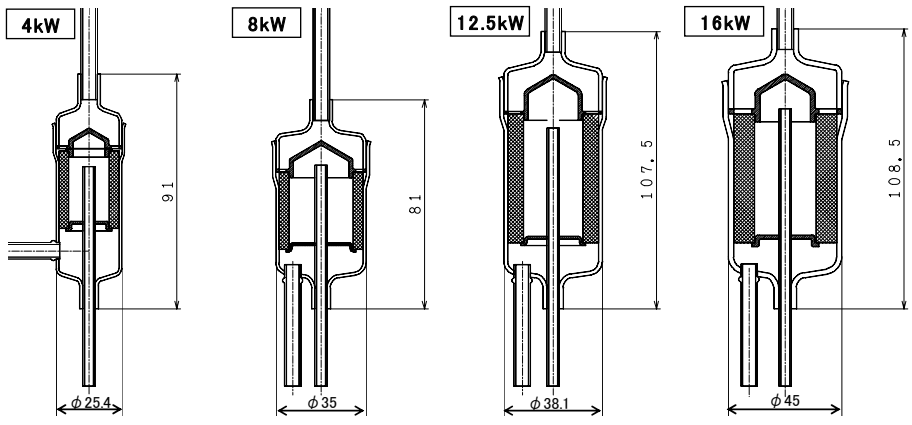


Fig. 12 Capacity variation

dimensionless correlation for the gas-liquid separation limit is obtained as follows:

$$Re_f^* = \min\left[1, 29.3We_G^{-1.486}\right] \quad (10)$$

By setting the gas and liquid flow rates within the border given by Eq. (10), perfect separation can be achieved.

## 3 GAS LIQUID SEPARATOR FOR R410A SYSTEMS

Figure 11 shows the configuration of the gas-liquid separator developed for R410A air conditioners. Gas-liquid separator designs from 4 to 16 kW air conditioners have been developed. Capacity variation designs are shown in Fig. 12. The volume of the separator is about 1/7 compared to the conventional separators.

Figure 13 shows the gas-bypass cycle in which gas-liquid separator is installed just upstream of the evaporator. The extracted gas is not introduced to the evaporator but by-passed directly to the compressor. Figure 14 shows the amount of liquid entrained to the gas by-pass route. As can be seen from the figure, less than 0.5% of the total liquid flow is entrained to the gas by-pass route. Based on the present separation performance, pressure drop of the evaporator is measured with and without the separator. The result is shown in Fig. 15. Pressure drop reduction of the evaporator is found to be more than 50%. It is thus confirmed that the present surface tension force based gas-liquid separator works very effectively in the real refrigeration cycles.

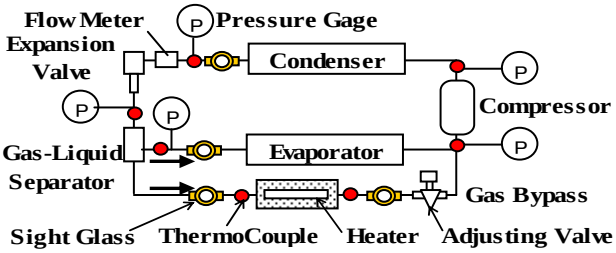


Fig. 13 Experimental setup

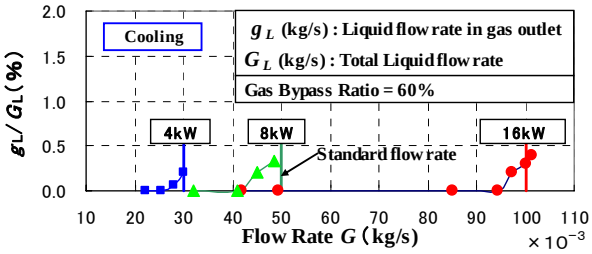


Fig. 14 Liquid entrainment to the gas outlet

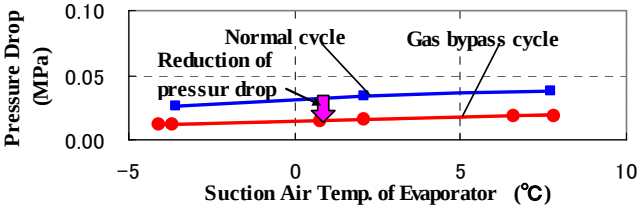


Fig. 15 Measured pressure drop reduction

## 4 CONCLUSIONS

A novel gas-liquid separator using surface tension is developed. Two gas-liquid separation limits, i.e., (1) flooding limit at high liquid flow rate, and (2) entrainment limit at high gas flow rate are found. Dimensionless correlations for predicting gas-liquid separation limits are proposed. Finally, a series of 4-16kW capacity gas-liquid separators for practical R410A air conditioning system are developed. The volume of the separator is about 1/7 compared to the conventional separators. Pressure drop reduction of the evaporator is demonstrated in the real R410A cycle.

## 5 REFERENCES

[1] Asano, H., Fujii, T., Takenaka, N. and Sakoda, K., A Study of the Phase Separation Characteristics in Gas-Liquid Two-Phase Flows by Impacting Y-Junction (1st Report, Experimental Results for Air-Water Two-Phase Flow under Normal Gravity Condition) , Transactions of the Japan Society of Mechanical Engineers, Series B, 67-654 (2001), 350-355.

[2] Asano, H., Fujii, T., Takenaka, N., Arakawa, T. and Suang, Y., A Study of the Phase Separation Characteristics in Gas-Liquid Two-Phase Flows by an Impacting Y-Junction (2nd Report, Experimental Results of the Effect of the Tube Diameter and Under Microgravity) , Transactions of the Japan Society of Mechanical Engineers, Series B, 68-673 (2002), 2542-2547.